sciendo

DOI: 10.2478/ata-2023-0022

Acta Technologica Agriculturae 3
Nitra, Slovaca Universitas Agriculturae Nitriae, 2023, pp. 166–172

USE OF DIGITAL IMAGE CORRELATION IN PREDICTING MECHANICAL PROPERTIES OF PARTS MADE BY ADDITIVE MANUFACTURING

Jakub PERNICA[1], Tomáš GAJDACZEK[1], Pavel ČERNÝ[1], Petr DOSTAL[1], Martin BRABEC[2], Maroš KORENKO[3]*

[1]Mendel University in Brno, Faculty of AgriSciences, Department of Technology and Automobile Transport, Brno, Czech Republic, jakub.pernica@mendelu.cz (J. P.), xgajdacz@mendelu.cz (T. G.), xcerny7@mendelu.cz (P. Č.), petr.dostal@mendelu.cz (P. D.)
[2]Mendel University in Brno, Faculty of Forestry and Wood Technology, Department of Wood Science, Brno, martin.brabec@mendelu.cz
[3]Slovak University of Agriculture in Nitra, Faculty of Engineering, Institute of Design and Engineering Technologies, Nitra, Slovak Republic
*correspondence: maros.korenko@uniag.sk

The publication is focused on the anisotropic properties of products of additive manufacturing using a Fused Filament Fabrication technology (FFF). Five different materials used in technical practice were tested. These materials are PLA (polylactic acid), PETG/CF (polyethylene terephthalate-glycol with carbon fibre, composite material), PETG (polyethylene terephthalate-glycol), ABS (acrylonitrile butadiene styrene), and ASA (acrylic styrene acrylonitrile). Mechanical properties are verified by tensile testing according to ASTM D638. Testing is complemented by a digital image correlation method to locate the areas with the highest load transfer. The results have shown clear anisotropic properties of the test specimens. Anisotropic mechanical properties were also confirmed by digital image correlation (DIC).

Keywords: mechanical properties; 3D print; polymer material; digital image correlation; material test

Additive manufacturing, or 3D printing, is a very broad term in current engineering practice. There are many technologies on the market that allow processing from polymer materials to various composite materials and metals (Hausman and Horne, 2014). It is a very dynamic developing manufacturing technology, whose advantages over traditional manufacturing methods include personalization (allowing the application of individual customer preferences), complexity (the possibility of internal structures to achieve the strength of load-bearing parts or, on the contrary, thin walls without filling to achieve low weight), sustainability (the use of environmentally friendly materials and optimisation of structures to reduce weight, for example in the aerospace industry), recycling and planned obsolescence (the possibility of producing non-available spare parts and the associated extension of product life), and economies of scale (since the production of jigs and moulds is eliminated, lower prices can be achieved when producing a small number of units). Additive manufacturing is characterised by creating a final three-dimensional object from a virtual 3D model by successively layering materials on the top of each other (Hausman and Horne, 2014). For this reason, products produced by 3D printing do not have a homogeneous structure and may exhibit different mechanical properties depending not only on the printing temperature, the height and width of the layer, but also on the orientation of the model in the 3D printer area (Weake et al., 2020). Fused Filament Fabrication (FFF) technology, in which the printing material (filament) is fused and layered, is currently one of the most affordable options for 3D printing polymers (Kloski and Kloski, 2017). At the same time, due to dynamic developments in engineering materials and additive manufacturing technologies, technical data that would enable wider use of 3D printing also in engineering practice are often lacking. This paper deals with the prediction of mechanical properties of printed parts in tension, as one of the important parameters in mechanical engineering. The main result of measurements is the determination of percentage decrease in tensile strength for products printed in the longitudinal and vertical direction in the printing area of a 3D printer (Průša and Bach, 2019). The aim of the paper is the unambiguous verification of the anisotropic properties of samples produced by additive manufacturing FFF in relation to the directional positioning of the samples in the printing area of the 3D printer. For the verification of anisotropic mechanical properties, an efficient digital image correlation (DIC) method was used for the tensile test.

Material and methods

Printing temperatures have a major influence on the quality of 3D printing. Each filament manufacturer specifies an optimal range of printing temperatures. These are the 3D printer bed and nozzle temperatures. The print temperature, especially the nozzle temperature, has a significant effect on the surface quality of prints. The temperature tower

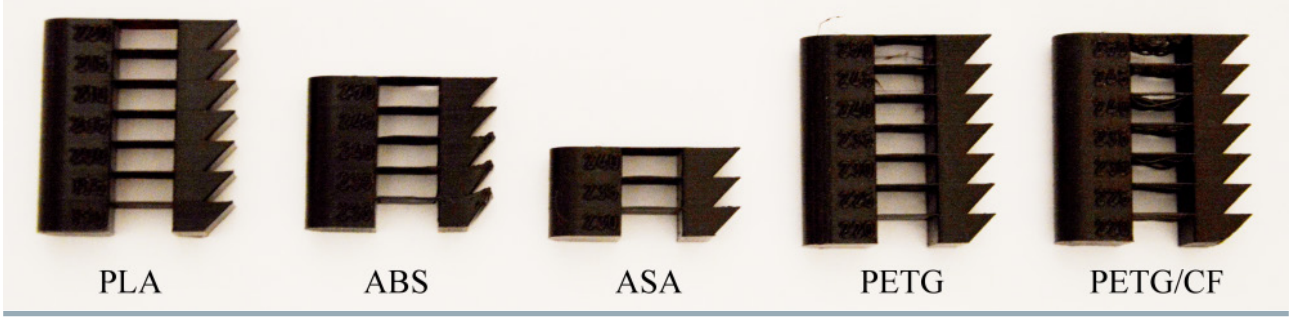


Fig. 1 Temperature towers

printing method was used to determine the optimum printing temperatures (Fig. 1). This is a method where the nozzle temperature is gradually increased. Temperature was increased gradually from the minimum temperature recommended by the manufacturer to the maximum recommended temperature. The nozzle temperature was increased in 5 °C increments. The nozzle temperature is always indicated directly on temperature towers (Hausman and Horne, 2014).

The evaluation of the test was done by sensory assessment of the quality of the prints. It was investigated at which temperature the filament starts to string (can be observed at high PETG material temperatures) and whether deformations occur (can be observed at low nozzle temperatures). The choice of final nozzle temperatures for printing the samples of each material was based on the experience gained in the field of 3D printing of polymer materials.

In addition to the parameters related to defining the samples themselves and printing temperatures, the parameters affecting the production process were also defined in PrusaSlicer in the 3D printer. These include defining the height of the print layer, the inner diameter of the nozzle, and print speed. Samples for all materials tested were made in accordance with ASTM D638 (Monzón et al., 2015). The sample series consists of five samples printed from the same material and in the same printing direction. Two samples from each 3D printing specification (material and 3D print direction) were selected for the DIC method and tested according to the ASTM D638 standard at a loading rate of 5 mm·min^{-1} by means of universal testing machine Tinius Olsen 10ST. The deformation of samples was captured by using the Digital Image Correlation (DIC) technique. To improve the robustness of image correlation during the DIC computation, the stochastic high contrast speckle pattern was applied on samples' surface. A thin matt white paint was covered by variously sized black speckle (Fig. 2).

The acquisition set consisted of two cameras AVT Stingray Copper F-504 B (the cell size of 3.45 µm and a resolution of 5 MPx), equipped with lenses Pentax C2514-M, with a focal length of 25 mm. The cameras were configured and calibrated into stereovision (3D) configuration. The resulted conversion factor was 15 Px·mm^{-1}. To enhance the contrast of the speckle pattern, the area of interest was illuminated by cold LED light sources Sobriety Cube 360 equipped with Luminus phlatlight CSM-360 LED chips. The images were acquired at a frequency of 4 Hz. Strain was calculated using of the lowest possible strain filter size of 5×5 Px in Vic-3D version 2010. The specimens that were not selected for digital image correlation measurements were tested using the standard ASTM D638 procedure of uniaxial tensile loading at a loading rate of 5 mm·min^{-1}. A total of fifty samples were tested by tensile testing according to ASTM D638. Twenty of these samples included DIC measurements. The remaining thirty samples were tested by the standard test. Tensile stress was calculated as the applied force divided by the solid cross section, regardless of internal porous structure of samples.

Table 1 Final nozzle temperatures for 3D printing of samples

Material	PLA	ABS	ASA	PETG	PETG/CF
Nozzle temperature (°C)	210	255	235	230	225

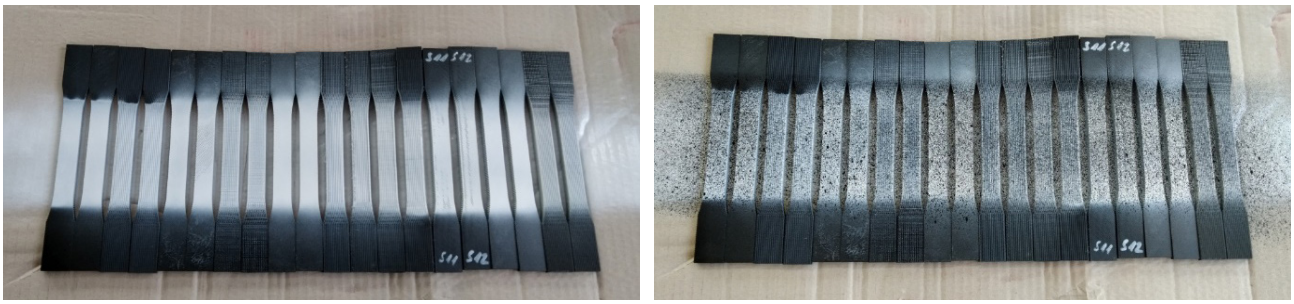


Fig. 2 Sample preparation process for DIC

Results and discussion

For samples L12, E11, and EC11, a high displacement concentration can be identified depending on the direction of each layer. Stress is concentrated in the direction of fibres ±45°. Sample A11 shows the highest stress concentration in the middle part of the sample. For this sample, a very good bonding of the layers or filaments of the print can be assumed. Specimen A11 also exhibited the greatest relative elongation of the tested specimens (Fig. 4).

Samples – vertical printing direction

Compared to the specimens that were printed in the longitudinal direction (Fig. 3), the specimens printed vertically (Fig. 4) exhibit a completely different tensile stress behaviour. The stress in the samples is concentrated in individual printed layers.

For samples L27, A26, and E26, stress is evenly distributed; therefore, the probability of failure is the same within the entire area of interest. Specimen S26 shows two areas of potential failure. These areas are a region in the middle and lower part of the stressed region. Due to the application of tensile stress in the smaller area, it can be assumed that the specimen breaks in the middle part. This prediction is confirmed by the location of actual specimen break (Fig. 3). Sample EC26 (PETG composite material with carbon admixture) shows a completely different behaviour. This sample shows large tensile stress variations in the measured region. Compared to the longitudinally printed specimens, the vertically printed specimens show a much smaller relative elongation.

For specimen EC11 (Fig. 5), a mirror reversed stress concentration can be observed compared to the breaking point of the specimen. This phenomenon is due to the reversed placement of the specimen in the testing machine.

Samples printed in the vertical direction, i.e., parallel to the *Z*-axis, show the fracture point as predicted by the DIC method (Fig. 6).

From the measured values, is it clear that the highest tensile strength of the PLA material printed in the longitudinal position is R_m = 38.14 ± 1.17 (MPa). On the other hand, the ASA material printed in the vertical position shows the lowest ultimate strength R_m = 5.09 ± 1.50 (MPa). An important result of measurements is a relatively high difference in tensile strength related to the orientation of the specimen on the substrate. This stress drop is 43.89 ± 3.17 (%) for the tested materials PLA, ABS, PETG, and PETG/CF. The largest difference was observed for the tested material ASA, where the decrease in ultimate tensile strength was almost 85%. Stress-strain diagrams were further developed from the measured values. The samples printed in the longitudinal direction are compared in Fig. 7. When compared with the stress strain diagram (Fig. 8) created for samples printed in the vertical orientation of samples in the printing area of the 3D printer, there is a significant difference in the tensile strength region. Samples printed in the longitudinal direction show a parabolic pattern in

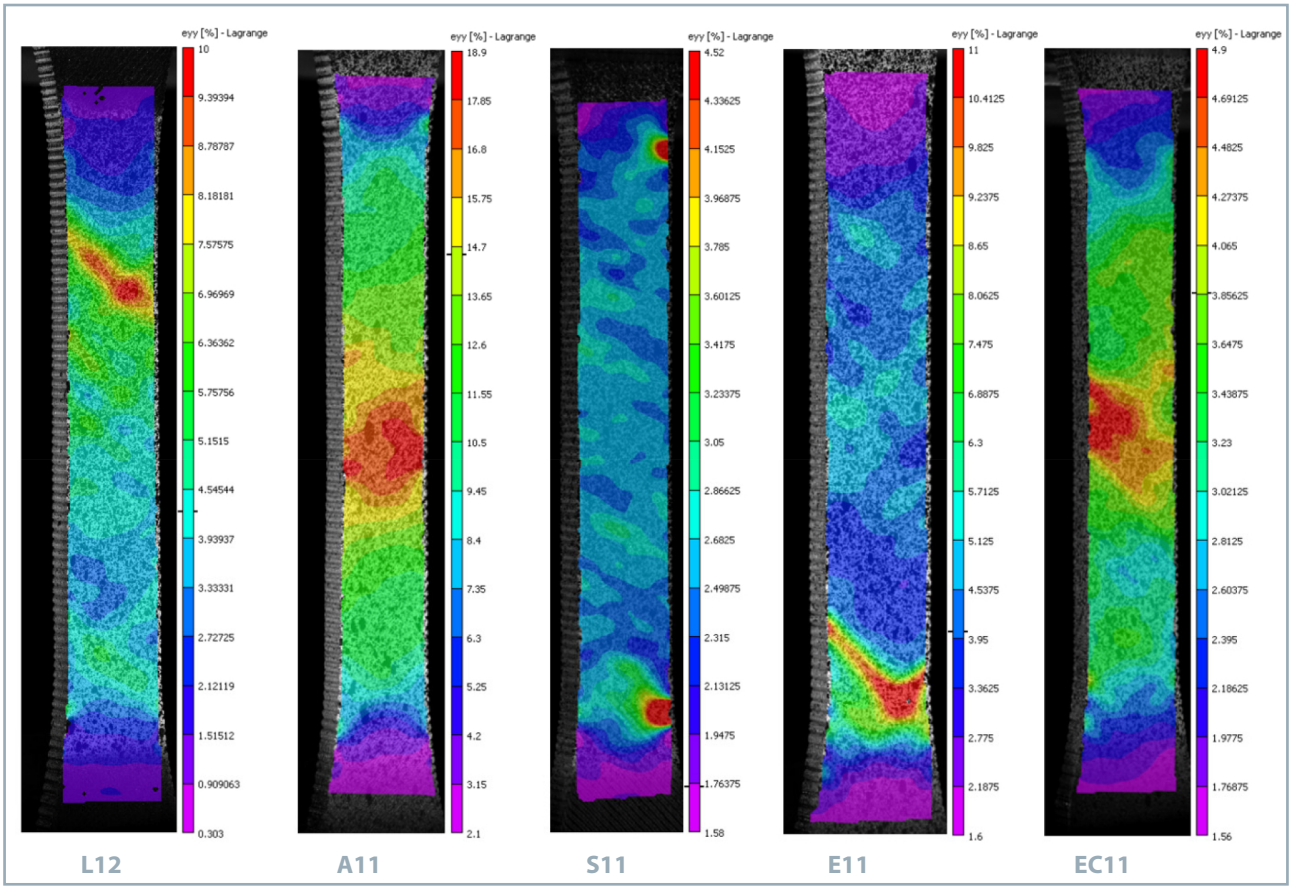


Fig. 3 DIC – longitudinal direction of printing

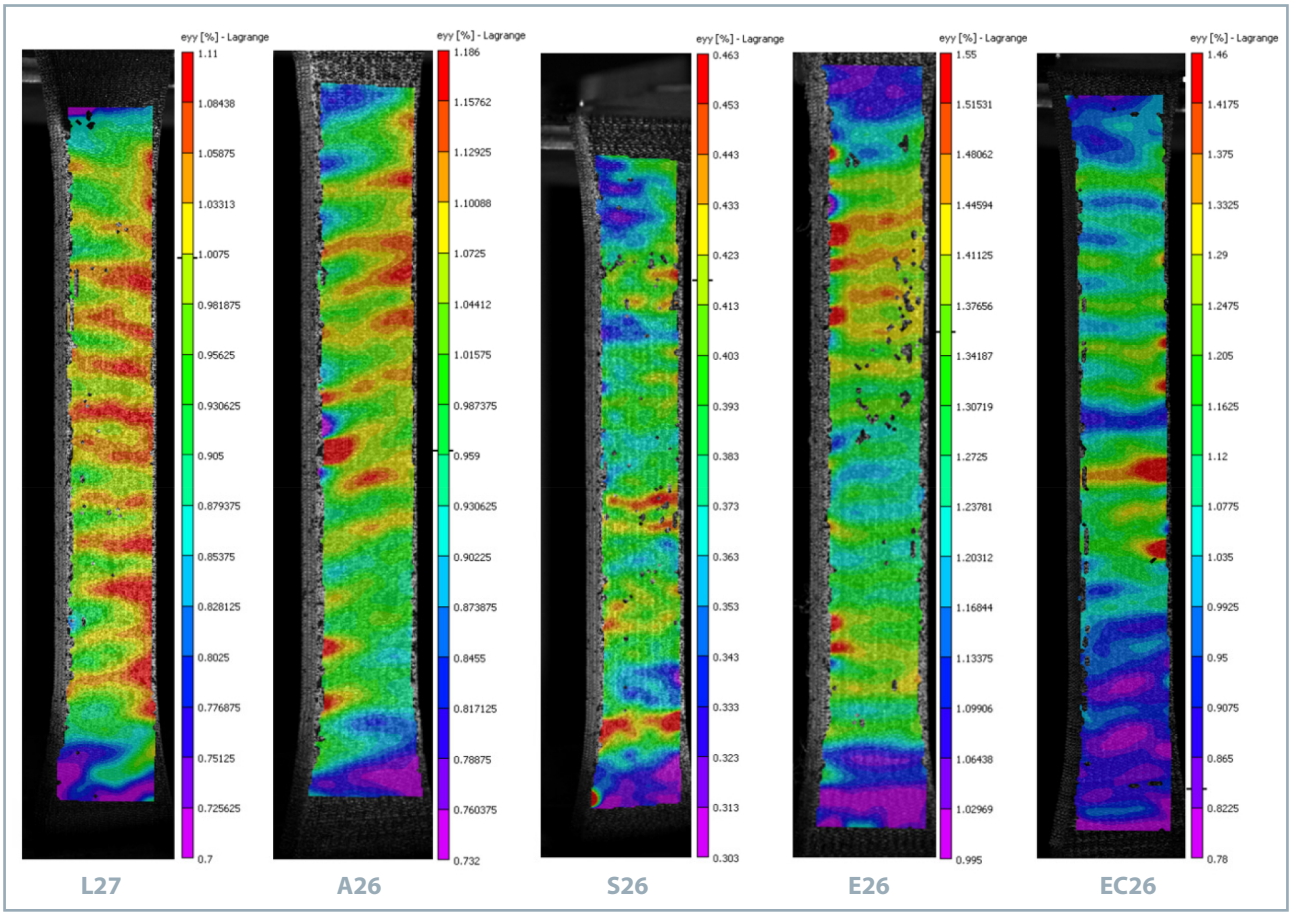


Fig. 4 DIC – vertical printing direction

the region of the maximum tensile forces. Samples printed in the vertical orientation in the print space show a linear pattern and exhibit a sharp drop in stress in the region of the maximum stress. It can therefore be predicted that for prints loaded with normal forces on the lay-up direction, it will be very difficult to identify the critical condition of the print in operation.

The measured values (tensile strength) of all tested specimens were finally processed into box plots. Box plots were chosen because of the statistical evaluation of the strength limits of tested specimens. The main reason for creating them was to verify statistically significant differences in the values found.

Figure 9 shows that there are statistically significant differences in tensile strength between the materials tested. The largest difference was observed between the PLA and PETG/CF materials. On the other hand, no statistically significant difference was found between the specimens

Table 2 Tensile strength of tested materials

Material	Group of samples	Directions of 3D printing	Tensile strength (MPa)	Standard deviation (MPa)	Drop in tensile strength longitudinal → vertical orientation of 3D printing (%)
PLA	L11–L15	longitudinal	38.14	±1.17	-40.99
	L26–L30	vertical	22.51	±2.68	
ABS	A11–A15	longitudinal	31.18	±1.09	-46.79
	A26–A30	vertical	16.59	±2.30	
ASA	S11–S15	longitudinal	33.77	±1.13	-84.92
	S26–S30	vertical	5.09	±1.50	
PETG	E11–E15	longitudinal	35.28	±1.27	-46.93
	E26–E30	vertical	18.72	±1.51	
PETG/CF	EC11–EC15	longitudinal	28.46	±2.47	-40.08
	EC26–EC30	vertical	17.05	±1.07	



Fig. 5 Selected samples after failure – printing in the longitudinal direction

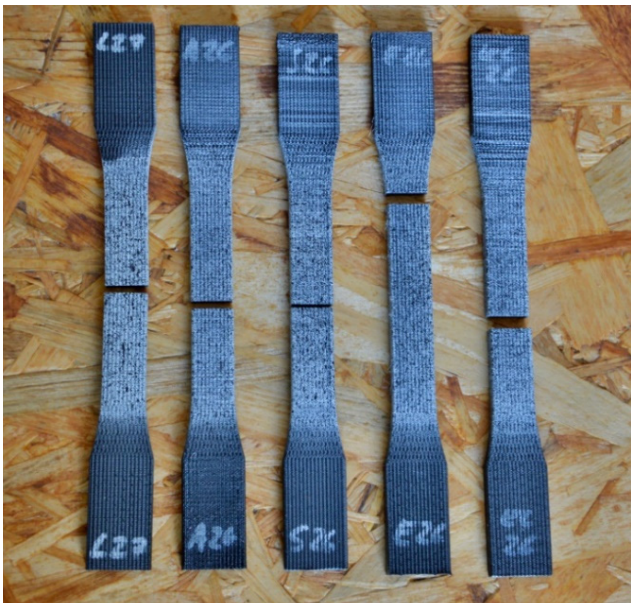


Fig. 6 Selected specimens after failure – printing in the vertical direction

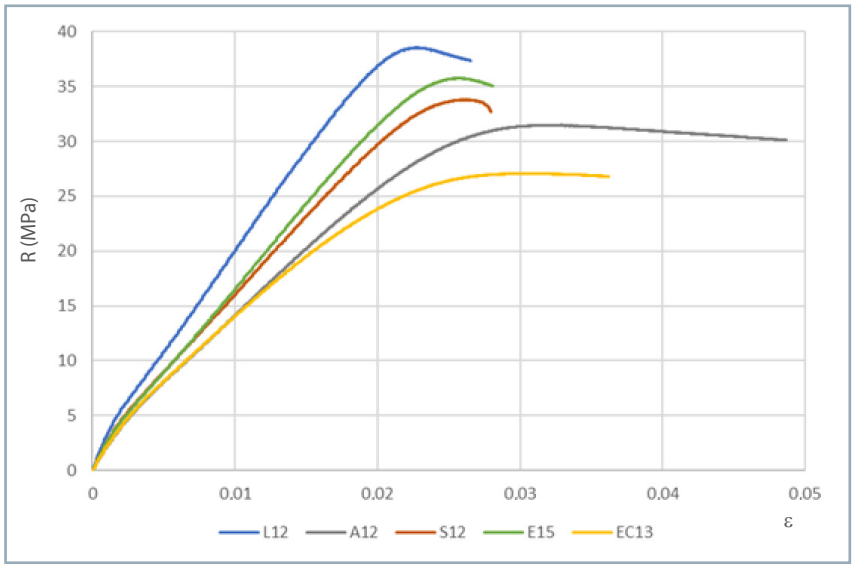


Fig. 7 Tensile diagram of the tested materials printed in the longitudinal direction

made from the ASA and PETG materials. A similar result was also observed between the samples made of ABS and PETG/CF. The results of the tensile strength of tested specimens made of the ABS material show similar limit values to those reported by (Czyżewski et al., 2018). Compared, for example, to metal materials, specifically stainless steel, the samples printed in the longitudinal direction show tensile strength values less than one-tenth of a percent (Poláková and Dostál, 2019).

Figure 10 shows that the largest statistically significant difference was observed between samples that were printed from the PLA and ASA materials. The difference in median ultimate strength for the pair of materials mentioned is 17.79 MPa. There was a significant difference between the samples made from the ABS, PETG, and PETG/CF materials.

When comparing Fig. 9 and Fig. 10, it was shown that there is a statistically significant difference in tensile strength between the two groups of specimens tested. When comparing the median of the specimens exhibiting the highest and lowest tensile strength values, a difference of 32.87 MPa was found. This is a comparison of the group of samples made of the PLA material (longitudinal printing direction) and the samples made of the ASA

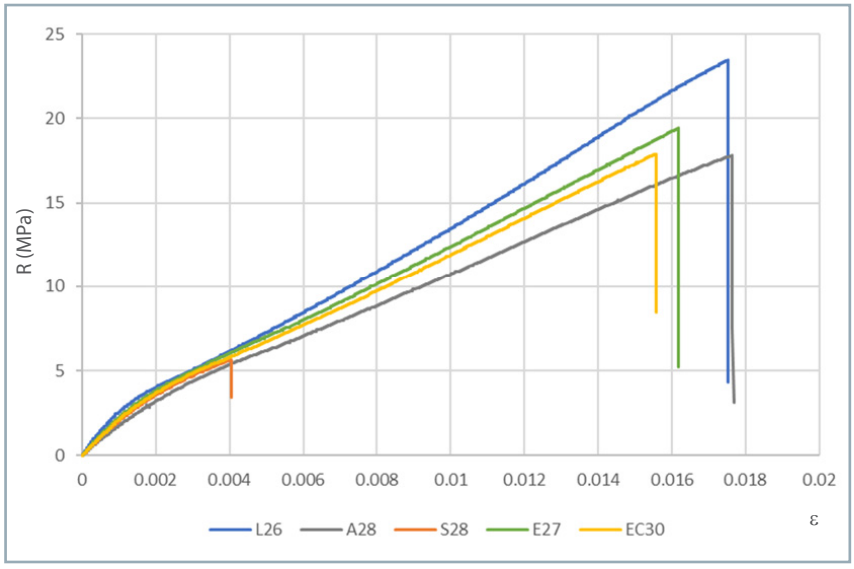


Fig. 8 Tensile diagram of samples printed in the vertical direction

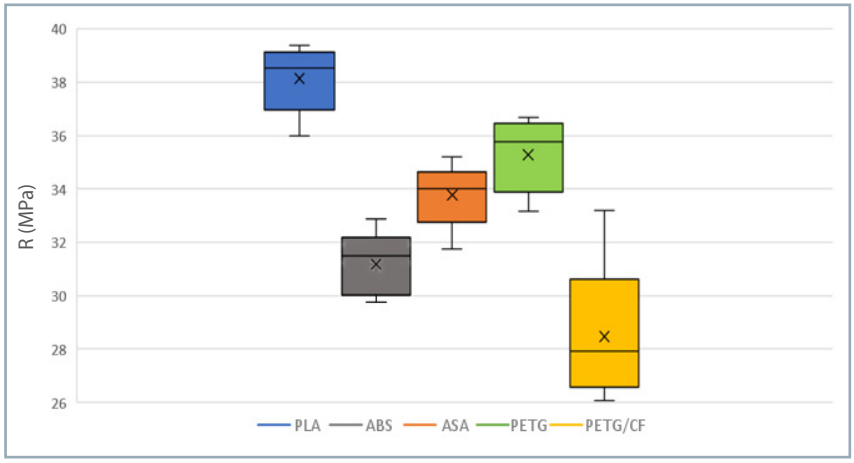


Fig. 9 Box plot – specimens printed in the longitudinal direction (parallel to the *X*-axis)

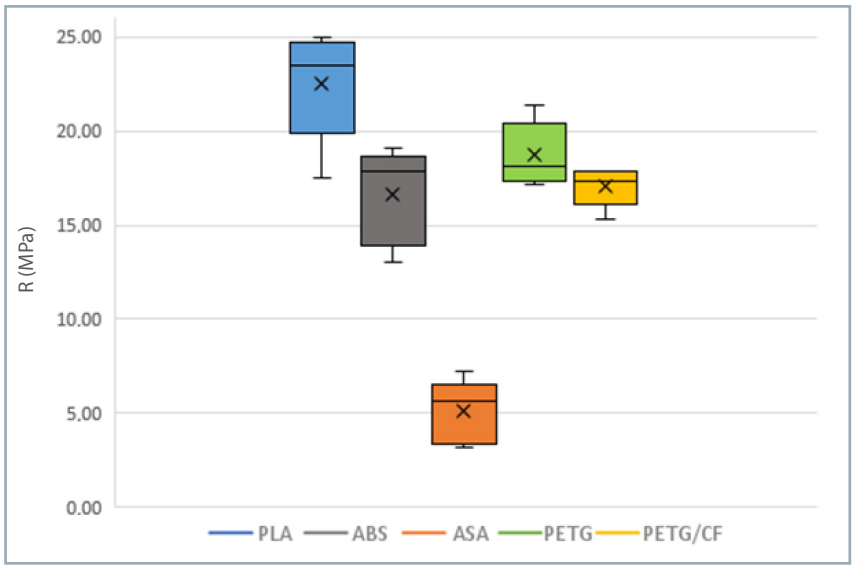


Fig. 10 Box plot – specimens printed vertically (parallel to the *Z*-axis)

material (vertical printing direction). In comparison with composite materials, samples made with PETG materials printed vertically can be most closely compared with biocomposites with the specification Green HDPE/Woven sisal fibres in 0°/90° (De Castro et al., 2020). The difference of the mentioned groups of samples approximately corresponds to the measured median tensile strength of the samples that were printed from the ABS material in the longitudinal direction (parallel to the *X*-axis).

Conclusion

The effect of 3D model placement in space and the specification of the 3D printing process has a significant impact on the mechanical properties of products. In particular, anisotropic mechanical properties are manifested (Koch et al., 2017). The measurements confirmed the assumption that the orientation of the sample in the 3D printer print space has a direct influence on the strength parameters of printed samples. The same results are reported by Lokesh et al. (2022). The filling of samples was set to 100% and a grid was chosen for the filling type. The measurements were extended with the digital image correlation method. From the results of measurements on the universal tearing machine with the extension of the above method, it was possible to define the areas with the highest stress concentration. The results of digital image correlation measurements were confirmed by comparing the physically torn samples with digital image correlation results. The DIC method can be used not only for the tested materials used in additive manufacturing (Zaldivar et al., 2017). From the DIC results, it is also possible to unambiguously demonstrate anisotropic properties due to the orientation of samples in the printing space of the 3D printer (Pellegrini et al., 2022).

Acknowledgement

The research has been supported by the project AF-IGA2022-IP-054 Optimization of heat treatment methodology of additive manufacturing products.

References

ASTM D638: 2010. Standard test method for tensile properties of plastics. ASTM Internatio nal, West Conshohocken, PA, USA.

CZYŻEWSKI, P. – BIELIŃSKI, M. – SYKUTERA, D. – JUREK, M. – GRONOWSKI, M. – RYL, Ł. – HOPPE, H. 2018. Secondary use of ABS co-polymer recyclates for the manufacture of structural elements using the FFF technology. In Rapid Prototyping Journal, vol. 24, no. 9, pp. 1447–1454.

DE CASTRO, B. D. – DE FARIA, P. E. – VIEIRA, L. M. G. – RUBIO, C. V. C. – MAZIERO, R. – DE MATOS RODRIGUES, P. C. – RUBIO, J. C. C. 2020. Recycled green PE composites reinforced with woven and randomly arranged sisal fibres processed by hot compression moulding. In Acta Technologica Agriculturae, vol. 23, no. 2, pp. 81–86. DOI: https://doi.org/10.2478/ata-2020-0013

HAUSMAN, K. K. – HORNE, R. 2014. 3D Printing for Dummies. New Jersey : John Wiley, 384 pp. ISBN 978-1-118-66075-1

KLOSKI, L. W. – KLOSKI, N. 2017. Starting with 3D printing (In Czech: Začínáme s 3D tiskem). Brno : Computer Press, 211 pp. ISBN 978-80-251-4876-1.

KOCH, C. – VAN HULLE, L. – RUDOLPH, N. 2017. Investigation of mechanical anisotropy of the fused filament fabrication process via customized tool path generation. In Additive Manufacturing, vol. 16, pp. 138–145. DOI: https://doi.org/10.1016/j.addma.2017.06.003

LOKESH, N. – PRAVEENA, B. A. – SUDHEER, R. J. – VIKRAM, K. V. – VIJAYKUMAR, S. 2022. Evaluation on effect of printing process parameter through Taguchi approach on mechanical properties of 3D printed PLA specimens using FDM at constant printing temperature. In Materials Today: Proceedings, vol. 52, no. 3, pp. 1288–1293. DOI: https://doi.org/10.1016/j.matpr.2021.11.054

MONZÓN, M. D. – ORTEGA, Z. – MARTÍNEZ, A. – ORTEGA, F. 2015. Standardization in additive manufacturing: activities carried out by international organizations and projects. In The International Journal of Advanced Manufacturing Technology, vol. 76, no. 5–8, pp. 1111–1121. DOI: https://doi.org/10.1007/s00170-014-6334-1

PELLEGRINI, A. – PALMIERI, M. E. – GUERRA, M. G. 2022. Evaluation of anisotropic mechanical behaviour of 316L parts realized by metal fused filament fabrication using digital image correlation. In The International Journal of Advanced Manufacturing Technology, vol. 120, no. 11–12, pp. 7951–7965.
DOI: https://doi.org/10.1007/s00170-022-09303-z

POLÁKOVÁ, N. – DOSTÁL, P. 2019. Titanium and stainless steel MIG LSC welding. Acta Technologica Agriculturae, vol. 22, no. 2, pp. 56–59. DOI: https://doi.org/10.2478/ata-2019-0010

PRŮŠA, J. – BACH, M. 2019. The Basics of 3D Printing. Praha : Prusa Research, 61 pp. Available at:
https://www.prusa3d.cz/kniha-zaklady-3d-tisku-josefa-prusi/ (In Czech: Základy 3D tisku)

WEAKE, N. – PANT, M. – SHEROAN, A. – HALEEM, A. – KUMAR, H. 2020. Optimising process parameters of fused filament fabrication to achieve optimum tensile strength. In Procedia Manufacturing, vol. 51, pp. 704–709.
DOI: https://doi.org/10.1016/j.promfg.2020.10.099

ZALDIVAR, R. J. – WITKIN, D. B. – MCLOUTH, T. – PATEL, D. N. – SCHMITT, K. – NOKES, J. P. 2017. Influence of processing and orientation print effects on the mechanical and thermal behavior of 3D-Printed ULTEM® 9085 material. In Additive Manufacturing, vol. 13, pp. 71–80.